INTERNATIONAL JOURNAL OF INTELLIGENT CONTROL AND SYSTEMS
VOL. 13, NO. 1, MARCH 2008, 25-37

Intelligent Control of Dynamic Target Tracking of a Car-Like Wheeled Robot in a Sensor-Network Environment

Chih-Lyang HWANG, Tsai-Hsiang WANG and Ching-Chang WONG

Abstract -- **In this paper, the dynamic target tracking of a car-like wheeled robot within a sensor-network environment by an intelligent control is developed. The proposed intelligent control is called fuzzy decentralized sliding-mode grey prediction control (FDSMGPC). For implementing dynamic target tracking, two distributed CCD (charge-coupled device) cameras are set up to capture the poses of the tracking and target cars, which have the front-wheel for the steering orientation and the rear-wheel for the translation motion. Based on the control authority of these two CCD cameras, a suitable reference command for the proposed controller of the tracking car is planned on a personal computer and then transmitted to the tracking car by a wireless device. The reference command contains the reference steering angle of the front-wheel and the reference velocity of the rear-wheel. Only the information of the upper bound of system knowledge is required to select the suitable scaling factors and the coefficients of sliding surface for the proposed controller. Since the target car is dynamic and the tracking car possesses dynamics, a grey prediction for the pose of the target car is employed to plan an *effective* reference command. Finally, a sequence of experiments confirms the usefulness of the proposed control system.**

Index Terms: **Sensor-network environment, Target tracking, Car-like wheeled robot, Fuzzy decentralized sliding-mode control, Grey prediction.**

1. INTRODUCTION

Recently, distributed control applications within sensor networks are gaining a role of importance (e.g., [1-4]). Such sensor-network environments are able to monitor what is occurring themselves, to build their own models, to communicate with their inhabitants, and to act on the basis of decisions they make. In addition, many of the problems encountered by classic wheeled robots (e.g., localization [5], high computational power [6-8], different software for different kinds of mobile robot [9, 10], the interference with each sensor [10]) are solved when they are in a sensor-network environment. The so-called sensor-network environment consists of the objects inside of this space that can be detected by different CCD cameras. The area simultaneously observed by two CCD cameras is an over-lapped region to completely monitor the interesting objects. In order to catch the synchronous images, a set of synchronizers is installed. Based on the concept of sensor-network environment (e.g., [1-4]), two distributed CCD cameras are employed to provide the pose of the tracking and target cars (see Table 1 for the specifications). If the monitoring region is larger, the number of the CCD cameras should be increased or active CCD cameras should be considered [11]. After the image processing in a personal computer, the poses (i.e., position and orientation) of the tracking and target cars are applied to plan a reference command for the controller of the tracking car. This on-line planning trajectory is then transmitted to the tracking car by a wireless device.

Because the decentralized control scheme is free from the difficulties arising from the complexity in design, debugging, data gathering, and storage requirements, it is more preferable for a tracking car than a centralized control [12, 13]. As one knows, a fuzzy control algorithm [14-16] consists of a set of heuristic decision rules and is regarded as a nonmathematical control algorithm. It has been proved to be attractive whenever the controlled systems cannot be well defined or modeled. However, a trial-and-error design approach is typically required to obtain an acceptable tracking performance. In this situation, the combination of the sliding-mode control and fuzzy control so-called fuzzy sliding-mode control (FSMC) provides a robust controller for the nonlinear systems [17, 18]. The differences between the fuzzy sliding-mode control and classic fuzzy control are summarized as follows: (i) The coefficients of sliding surface in FSMC can shape the frequency of the closed-loop system; however, classic fuzzy control does not have this feature. Then the bandwidth of the tracking car can be appropriately assigned to avoid a sluggish or oscillatory response ([19] or *Remark* 3 of subsection 3.1). (ii) Because the sliding-mode control possesses the invariance property [17, 18], disturbance immunity of the FSMC is better than that of classic fuzzy control as the operating point is on the sliding surface. In short, the robustness of the FSMC is better than that of classic fuzzy control. (iii) The adjustment of control parameters for the FSMC is easier than that of classic fuzzy control. There are *five* control parameters for the FSMC. Two coefficients are first set to obtain the suitable dynamics of the sliding surface, which is the linear combination of present and past tracking error. Based on the practical ranges of the sliding surface and its derivative, two normalizing scaling factors are chosen.

Manuscript received October 31, 2007; revised February 8, 2008. This work was supported by NSC of Taiwan, R.O.C. under Grant No. NSC-94-2213-E-036-003. This paper is extended from "A dynamic target tracking of wheeled robot in sensor-network environment via fuzzy decentralized sliding-mode grey prediction control," *IEEE ICRA2007*, Roma, Italy, Apr. 2007.

Chih-Lyang Hwang and Ching-Chang Wong are with the Department of Electrical Engineering of Tamkang University, Taipei County, Tamsuei, Taiwan (email: clhwang@mail.tku.edu.tw, wong@ee.tku.edu.tw) .

Eventually, the fifth parameter is the output scaling factor, which is chosen according to the system stability. No trial-and-error is needed. (iv) The stability proof of FSMC is more easily derived than that of classic fuzzy control.

Based on the above analysis, the fuzzy rule table of the *ith* subsystem using sliding surface and its derivative (i.e., the set of if-then rules) is achieved. Then the quantity of this fuzzy table is assigned as the value between -1 and 1 (see *Remarks* 1 and 2 of subsection 3.1). This fuzzy table is skew-symmetric about the diagonal line; its absolute value is proportional to the distance from the diagonal line. Based on the system stability, the output scaling factor for the crisp control input, which is equal to the value determined from the fuzzy table multiplying the output scaling factor, is selected. Generally speaking, a larger output scaling factor is assigned, a smaller tracking error and a faster response are obtained; however, the risk of transient response occurs. Then a saturation of control input will result in a possible instability.

The proposed control can track a reference command without the requirement of a mathematical model. Only the information of the upper bound of the tracking car is needed to choose suitable coefficients of sliding surface and scaling factors such that a satisfactory performance is obtained. Because the target car is dynamic and the tracking car also possesses dynamics, a prediction of the pose of the target car is required to improve the tracking performance. Most of the existing approaches need a *priori* kinematics model of the target car for the prediction. Although this predictor can successfully filter out the noisy measurement, its parameters might be changed due to different dynamic targets. In addition, the exact dynamic models of tracking and target cars are either difficult to obtain or need complex mathematical descriptions (e.g., [6, 20]). Because a grey prediction is simple and effective [6, 21-23], a grey model is applied to predict the pose of the target car. Based on the predicted pose, a fuzzy decentralized sliding-mode grey prediction control (FDSMGPC) is then designed such that an improved tracking result is accomplished. Because the prediction merely provides a reference command, the stability of the proposed closed-loop system does not change. Finally, a sequence of experiments in a sensor-network environment is arranged to evaluate the effectiveness of the proposed control system. Although this paper discusses the navigation of indoor tracking and target cars, an outdoor application can be obtained if the CCD cameras are replaced by a global positioning system (GPS) [24]. In addition, part of this paper was published in the conference paper [25].

2. SYSTEM DESCRIPTION AND PROBLEM FORMULATION

There have two subsections in this section: one is system description, the other is problem formulation.

2.1 System Description

Fig. 1 shows the block diagram of the overall system in a sensor-network environment. The overall system includes a tracking car with a wireless device, a target car, two CCD cameras, and one personal computer, including an image processing card and a wireless device. For a tracking car with size and shape, its location in the 2-D Cartesian space can be uniquely determined by the spatial position (x, y) of the base point and the orientation angle θ with respect to the base point (see Fig. 2). Generally, the kinematics constraint of a nonholonomic mobile robot is described as follows (see, e.g., [26, 27]):

$$-\dot{x}(t)\sin\theta(t) + \dot{y}(t)\cos\theta(t) = 0 \,. \tag{1}$$

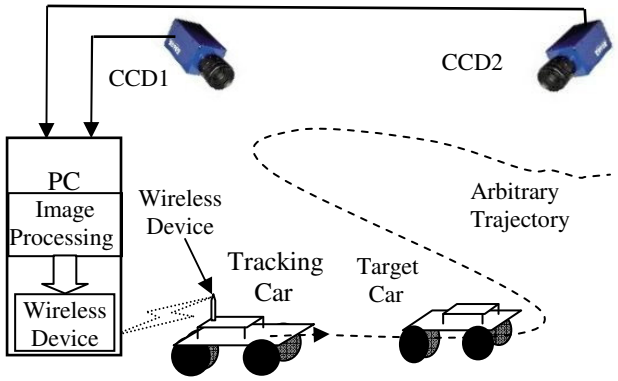

Fig. 1. The block diagram of the overall system.

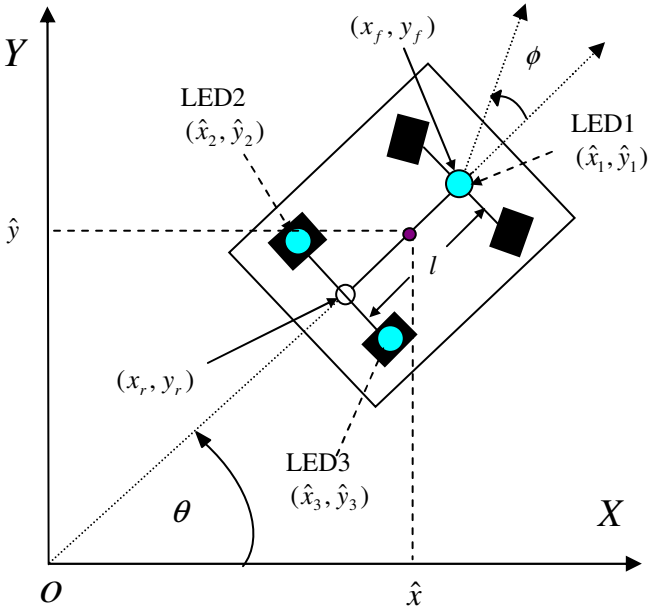

Fig. 2. Kinematics model and three locations of LED for a tracking car.

Without this constraint, the proposed CCD cameras in sensor-network environment can on-line detect the poses of tracking and target cars. Furthermore, the velocity parameters of the tracking car are expressed as follows:

$$\dot{x}_r(t) = v\cos(\theta), \dot{y}_r(t) = v\sin(\theta), \quad \text{and} \quad \dot{\theta}(t) = v\tan(\phi)/l \quad (2)$$

where (x_r, y_r) denotes the position of the rear-wheel center of the tracking car, $\theta(t)$ is the angle between the orientation of the tracking car and the *X*-direction, ϕ is the orientation of the steering wheel with respect to the frame of the tracking car, v denotes the speed of the longitude (or rear-wheel), and l is the wheelbase of the tracking car. Similarly, the kinematics model of the front-wheel of the tracking car is the same as (2).

The experimental setup of the tracking car is depicted in Fig. 3. Except for a wireless device, the target car is the same as the tracking car. The mechanism design of the tracking car is according to Ackerman principle. Thus, the tracking car rotates along the single transformation center (i.e., point D in Fig. 3(b)) in changing direction to go on so that the wheel can totally roll smoothly. During the turning of the tracking car, a line vertically passing through point D is the rotation axis for the extension lines of two front-wheels and the extension line of the rear-wheel shaft. In this paper, the servo control system of the tracking car includes two DC motors from Maxon Co., one digital signal processor (DSP of TMS320LF2407 from TI Co.), one driver, a 12-bits DAC using AD7541A, and one wireless device SST-2450 spread spectrum radio modem with controlling an RS-232/RS-485 interface port (see Fig. 3(c)). The rear-wheels are fixed parallel to the car chassis and allowed to roll or spin but are assumed to roll without slipping; two front-wheels are parallel and can simultaneously turn to the right or left. Front-wheel and rear-wheel are individually driven by the same permanent magnet DC motor. Finally, the basic specifications of the tracking car are shown in Table 1.

Table 1. Basic specifications of tracking car.

Car-Like Wheeled Robot	Length	400*mm*
	Width	240*mm*
	Height	200*mm*
	Weight	3.5 *kg*
Front-Wheel (Steering Wheel)	Diameter	110*mm*
	Thickness	45*mm*
	Wheelbase	240*mm*
Rear-Wheel (Drive Wheel)	Diameter	110*mm*
	Thickness	45*mm*
	Wheelbase	270*mm*
Height of Chassis	20*mm*	

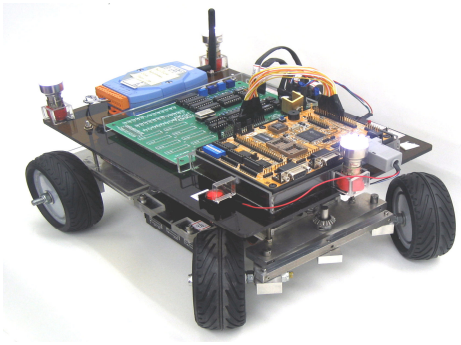

(a) Photograph.

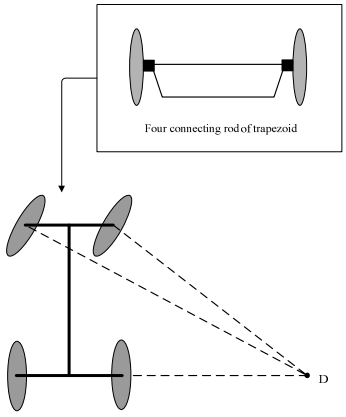

(b) Mechanism design using Ackerman principle.

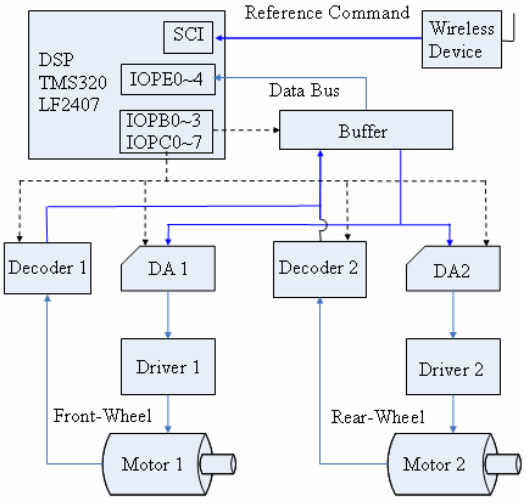

(c) Block diagram of servo control system.

Fig. 3. Experimental setup of the tracking car.

The Matrox Meteor-II card is applied as an image processing card. It is a monochrome and RGB component

analog frame grabber for standard and non-standard video acquisition. It is also available in a PCI or PC/104-Plus form factor, both of which can use a Matrox Meteor-II MJPEG module for compression and decompression of monochrome and color images. The board features six software-selectable input channels on which two components RGB or six monochrome cameras can be attached. It supports acquisition from one camera at a time or simultaneous acquisition from up to three RS-170/CCIR cameras (i.e., RS-170RGB); it supports both single and dual-tap configurations. It also accepts an external trigger, and can operate in either asynchronous reset mode or next valid frame/field mode. The software Matrox MIL-Lite 6.0 developed by Matrox possesses many modules, which can be used to recognize image.

2.2 Problem Formulation

The so-called sensor-network environment consists of the objects inside of this space that can be detected by different CCD cameras. An overlapped region, simultaneously observed by two CCD cameras, is designed for *completely* monitoring the interesting objects. In order to catch the synchronous images, a set of synchronizers is installed. To distinguish the tracking car and the target car, two sets of three LEDs with different light area are respectively applied to the tracking car and the target car (see subsection 4.1 for the details). After the image processing, the poses of tracking and target cars are accomplished. Then the reference commands, including the reference steering angle for the front-wheel and the reference translation velocity for the rear-wheel of the tracking car, are planned and transmitted by wireless device. The software used to implement the work described in this paper includes: (i) the Code Composer for editing and downloading the control program to DSP, (ii) the FDSMCGPC algorithm in DSP written by C language, and (iii) various programs for (a) the image processing, (b) the transmission of a reference command from PC to DSP, (c) the decode of the position of the motor.

In the beginning, the FSMC is successfully applied to control a DC motor. Then two DC servo motors for the front-wheel and rear-wheel of the tracking car are controlled by individual FSMC. It is so-called fuzzy decentralized sliding-mode control (i.e., FDSMC). Although two DC motors are successfully controlled by FDSMC, the dynamics of the tracking car is different from that of the DC motor. In this situation, the dynamics of the two DC motors is in the presence of uncertainties. Only based on the results of DC motor, the performance of the tracking car is poor. This situation can be tackled by a modification of the scaling factor in the FDSMC such that a satisfactory robust performance is obtained. Because the target car is dynamic and the tracking car possesses dynamics, a grey prediction for the pose of the target car is employed to plan an *effective* reference command to improve the tracking performance of dynamic target.

Finally, the main goal of this study is to investigate the tracking car performance using FDSMGPC for the target tracking in a sensor-network environment. The experiments are categorized into the following three cases: (i) to track the target car moving with a curve "8" (without) using grey prediction, (ii) to track the same trajectory of part (i) using grey prediction for different initial time of the tracking car, and (iii) to track the same trajectory of part (i) using grey prediction for different initial pose of the tracking car. The first experiment is employed to confirm the improved tracking performance by grey prediction. The second experiment with different initial time is applied to validate the satisfactory tracking performance of dynamic target. On the other hand, the last one emphasizes different pose of tracking car to demonstrate the excellent tracking result using the proposed control.

3. FUZZY DECENTRALIZED SLIDING-MODE GREY PREDICTION CONTROL

There are two subsections for the controller design. The first subsection discusses the design of FDSMC. Then the grey prediction is introduced in the subsection 3.2.

3.1 Fuzzy Decentralized Sliding-Mode Control

Consider a tracking car with the following dynamic equation (see, e.g., [26, 27]):

$$A(\sigma)\ddot{\sigma}(t) + B(\sigma,\dot{\sigma}) + C(\sigma) + \Gamma(\sigma,\dot{\sigma},t) = DU(t) \qquad (3)$$

where $\sigma(t) \in \Re^2$ is the state vector of the tracking car, $A(\sigma) \in \Re^{2\times 2}$ denotes the inertia matrix of positive definite for any $\sigma(t)$, $B(\sigma,\dot{\sigma}) \in \Re^2$ comprises the centrifugal, Coriolis torques, $C(\sigma) \in \Re^2$ denotes the gravitational torque, $\Gamma(\sigma,\dot{\sigma},t)$ stands for the nonlinear time-varying uncertainties, $D \in \Re^{2\times 2}$ represents a control gain, and $U(t) \in \Re^2$ is the control torque. It is assumed that the dynamics of (3) is unknown. However, the upper bound of function from (3) is supposed to be known (allude to (9) and (10)).

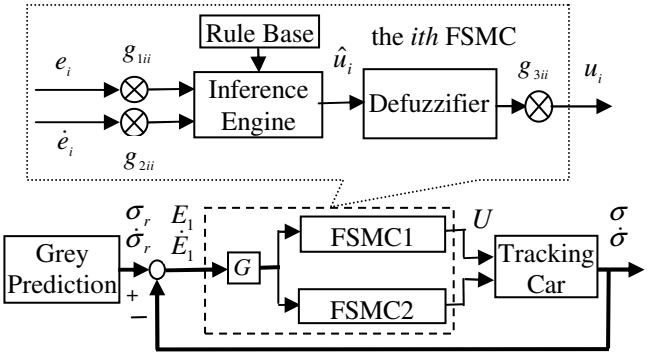

Fig. 4. Block diagram of the FDSMGPC for the tracking car.

The fuzzy logic subsystem *i* in Fig. 4 performs a mapping from $X_i \in \Re^2$ to $\Re$. There are *m* fuzzy control rules and the upper script *k* denotes the *kth* fuzzy rule:

$$\text{IF } \hat{s}_i(t) \text{ is } F_{1_i}^{\ k} \text{ and } \dot{\hat{s}}_i(t) \text{ is } F_{2_i}^{\ k} \text{ , THEN } \hat{u}_i(t) \text{ is } G_i^k \quad (4)$$

where $x_i(t) = \left[\hat{s}_i(t) \quad \dot{\hat{s}}_i(t)\right]^T \in X_i \subset \Re^2$ and $\hat{u}_i(t) \in V_i \subset \Re$ are the input and output of the fuzzy logic subsystem *i*, respectively; $F_{j_i}^{\ k} (1 \le i,\ j \le 2, 1 \le k \le m)$ and G_i^k are labels of sets in X_i and V_i, respectively. The fuzzy inference engine performs a mapping from fuzzy sets in $X_i \subset \Re^2$ to fuzzy sets in $V_i \subset \Re$, based upon the fuzzy IF-THEN rules in the fuzzy rule base and the compositional rule of inference. Let A_{x_i} be an arbitrary fuzzy set in X_i. The fuzzifier maps a crisp point $x_i(t)$ into a fuzzy set A_{x_i} in X_i. The center-average defuzzifier maps a fuzzy set in V_i to a crisp point in V_i [28]. The corresponding five control parameters $g_{1ii}, g_{2ii}, g_{sii}, g_{\dot{s}ii}$ and g_{3ii} are discussed later.

The FDSMC includes two sliding surfaces shown as follows:

$$S(t) = GE(t),\ G = \left[G_1 \quad G_2\right],\ E(t) = \left[E_1^T(t) \quad E_2^T(t)\right]^T \quad (5)$$

where $S(t) \in \Re^2$, $G_1 = diag(g_{1ii}) > 0, G_2 = diag(g_{2ii}) > 0 \in \Re^{2\times 2}$, $i = 1,2$ are the scaling factors, and

$$E_1(t) = \sigma_r(t) - \sigma(t),\ E_2(t) = \dot{E}_1(t) \quad (6)$$

where $\sigma_r(t) = [\sigma_{r_1}(t)\ \sigma_{r_2}(t)]^T = \left[\phi_r(t)\ v_r(t)\right]^T \in \Re^2$ is a reference trajectory for the tracking car, $E_1(t) = \left[e_1(t)\ e_2(t)\right]^T$, and $E_2(t) = \left[e_3(t)\, e_4(t)\right]^T$. From (3) and (6), it leads to

$$\dot{E}_2(t) = \ddot{\sigma}_r(t) - A^{-1}(\sigma)\left[DU(t) - B(\sigma,\dot{\sigma}) - C(\sigma) - \Gamma(\sigma,\dot{\sigma},t)\right] \quad (7)$$

The output of the FDSMC is designed as follows:

$$U(t) = G_3\hat{U}(t) = G_3\left[S(t) + \Delta \operatorname{sgn}(S)\right] \quad (8)$$

where $G_3 = diag(g_{3ii}) > 0 \in \Re^{2\times 2}$ is the output scaling factor, $\hat{U}(t)$ is fuzzy variable of $U(t)$, and $\Delta = diag(\delta_{ii}) > 0 \in \Re^{2\times 2}$. Suppose that

$$g_{3ii} \ge \left\{a_M d_M \left[\left|f_i(t)\right| + \lambda_i\right]\right\} / \left(g_{2m}\delta_{ii}\right) \text{ for } i = 1,2 \quad (9)$$

where $\lambda_i > 0, g_{2m} = \lambda_{\min}\{G_2\}, a_M = \lambda_{\max}\{A(\theta)\}, d_M = \lambda_{\max}\{D\}$, $f_i(t)$ is the *ith* element of the following vector:

$$\begin{aligned} F(t) &= G_1\left[\dot{\sigma}_r(t) - \dot{\sigma}(t)\right] \\ &+ G_2\left\{\ddot{\sigma}_r(t) + A^{-1}(\sigma)\left[B(\sigma,\dot{\sigma}) + C(\sigma) + \Gamma(\sigma,\dot{\sigma},t)\right]\right\}. \end{aligned} \quad (10)$$

The following theorem discusses the FDSMC for the partially known tracking car.

Theorem 1: Consider the unknown tracking car (3) with the known upper bound of (9), which is connected with the control parameters. Applying the control (8) with the satisfaction of condition (9) to the tracking car (3) gives the results (i) the finite time to reach the stable sliding surface (5), and (ii) the asymptotically tracking.

Proof: See *Appendix* for an abbreviated version of the proof.

Corollary 1: If the inequality (9) is satisfied outside of the following convex set:

$$D = \left\{S(t) \mid \left\|S(t)\right\| \le d_s\right\} \quad (11)$$

where d_s is a positive constant dependent on the upper bound of uncertainty, then $\{S(t), U(t)\}$ are uniformly ultimately bounded and the operating point reaches a convex set (11) in a finite time.

In addition, the brief introduction of FDSMC for the tracking car is given as the following three remarks.

Remark 1: It is assumed that $\dot{s}_i(t), i = 1,2$ increases as $u_i(t) = g_{3ii}\hat{u}_i(t)$ decreases; if $s_i(t) > 0$ then increasing $u_i(t)$ will result in decreasing $s_i(t)\dot{s}_i(t)$; and if $s_i(t) < 0$ then decreasing $u_i(t)$ will result in decreasing $s_i(t)\dot{s}_i(t)$. That is, the control input $u_i(t)$ is designed in an attempt to satisfy the inequality $s_i(t)\dot{s}_i(t) < 0$.

Remark 2: In the beginning, the fuzzy variable is quantized into the following seven qualitative fuzzy variables: (i) Positive Big (PB), (ii) Positive Medium (PM), (iii) Positive Small (PS), (iv) Zero (ZE), (v) Negative Small (NS), (vi) Negative Medium (NM), and (vii) Negative Big (NB). The inputs of fuzzy variable are defined as follows: $\hat{s}_i(t) = g_{iis}s_i(t)$ and $\dot{\hat{s}}_i(t) = g_{iis}\dot{s}_i(t)$, where $G_s = diag\{g_{11s}, g_{22s}\}$ and $G_{\dot{s}} = diag\{g_{11\dot{s}}, g_{22\dot{s}}\}$ are applied to normalize the values $\hat{s}_i(t)$ and $\dot{\hat{s}}_i(t)$ into the interval $[-1, 1]$. There are many types of membership functions, some of which are bell shaped, trapezoidal shaped, and triangular shaped, etc. For brevity, the triangular type in Fig. 5 is used in this application. The linguistic rule of the *ith* FDSMC is shown in Table 2 by which the center of gravity method is employed to form a look-up table in Table 3 that directly relates the inputs $\hat{s}_i(t)$ and $\dot{\hat{s}}_i(t)$ with the output $\hat{u}_i(t)$. In summary, the control actions of the diagonal terms are ZE. This arrangement is similar to a variable structure controller that has a sliding surface. In addition, the control actions of the upper triangle terms are from PS to PB, and those of the lower triangle terms are from NS to NB. This fuzzy table (i.e., Table 3) is skew-symmetric.

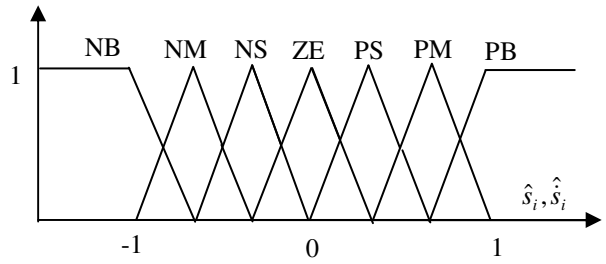

Fig. 5. Membership functions of triangular shape.

Table 2. Rule table of the *ith* FSMC.

s_i \ $\dot{s}_i$	PB	PM	PS	ZE	NS	NM	NB
NB	ZE	NS	NM	NB	NB	NB	NB
NM	PS	ZE	NS	NM	NB	NB	NB
NS	PM	PS	ZE	NS	NM	NB	NB
ZE	PB	PM	PS	ZE	NS	NM	NB
PS	PB	PB	PM	PS	ZE	NS	NM
PM	PB	PB	PB	PM	PS	ZE	NS
PB	PB	PB	PB	PB	PM	PS	ZE

Remark 3: The guideline for the selection of the five control parameters is addressed as follows. (i) Based on the inequality (9), the output scaling factor g_{3ii} is determined. First, it is chosen from a small value. According to the response, a larger value is then applied to improve the system performance. A larger output scaling factor is selected, a smaller tracking error is achieved; however, the risk of transient (or unstable) response occurs due to the constraints of the (rate of) control input.(ii) The parameters g_{sii} and $g_{\dot{s}ii}$ are chosen such that $\hat{s}_i(t)$ and $\dot{\hat{s}}_i(t) \in [-1,1]$. (iii) The dynamics of the sliding surface should not faster than that of reaching phase [17, 18]. That is, $-\lambda\{g_{1ii}/g_{2ii}\} < \gamma g_{3ii}$, where γ is a suitable and positive constant. (iv) The smaller $-\lambda\{g_{1ii}/g_{2ii}\}$ is set, the narrower bandwidth of the switching surface is assigned. Then the higher frequency component of the tracking error is filtered. However, the response of the trajectory tracking becomes more sluggish.

Table 3. Look-up table of the *ith* FSMC.

$\hat{s}_i$ \ $\dot{\hat{s}}_i$	1.0	0.8	0.6	0.4	0.2	0	-0.2	-0.4	-0.6	-0.8	-1.0
-1.0	0.0	-0.2	-0.4	-0.6	-0.7	-0.8	-0.9	-0.95	-1.0	-1.0	-1.0
-0.8	0.2	0.0	-0.2	-0.4	-0.6	-0.7	-0.8	-0.9	-0.95	-1.0	-1.0
-0.6	0.4	0.2	0.0	-0.2	-0.4	-0.6	-0.7	-0.8	-0.9	-0.95	-1.0
-0.4	0.6	0.4	0.2	0.0	-0.2	-0.4	-0.6	-0.7	-0.8	-0.9	-0.95
-0.2	0.7	0.6	0.4	0.2	0.0	-0.2	-0.4	-0.6	-0.7	-0.8	-0.9
0	0.8	0.7	0.6	0.4	0.2	0.0	-0.2	-0.4	-0.6	-0.7	-0.8
0.2	0.9	0.8	0.7	0.6	0.4	0.2	0.0	-0.2	-0.4	-0.6	-0.7
0.4	0.95	0.9	0.8	0.7	0.6	0.4	0.2	0.0	-0.2	-0.4	-0.6
0.6	1.0	0.95	0.9	0.8	0.7	0.6	0.4	0.2	0.0	-0.2	-0.4
0.8	1.0	1.0	0.95	0.9	0.8	0.7	0.6	0.4	0.2	0.0	-0.2
1.0	1.0	1.0	1.0	0.95	0.9	0.8	0.7	0.6	0.4	0.2	0.0

3.2 Grey Prediction

Because the target car is dynamic and the tracking car possesses dynamics, a prediction using grey theory is employed to forecast the future pose of the target car, which is used for the planning of the reference commands including the steering angle of the front-wheel and the velocity of the rear-wheel. Under this circumstance, the control performance based on a future pose of the target car can be enhanced. Because the prediction merely provides a reference command, the stability of the closed-loop system does not change.

The proposed method for the pose prediction of the target car is based on the grey theory [21-23], that assumes the internal structure, parameters, and characteristics of an observed system are unknown, or the so-called "black system." According to the pose estimation of the target car by two CCD cameras, an appropriate model is assigned to approximate its dynamics. The approximate model is the so-called "white system." Based on grey theory, the optimal parameters of the white system can be calculated. Generally, the grey model is written as $GM(\alpha,\beta)$, where α is the order and β is the number of variables of the modeling equation. The higher α is assigned, the more sensitive to the input data will the obtained model become. Among the GM family, the first-order one-variable grey model, i.e., *GM* (1, 1), is most widely used and is successfully demonstrated in many applications such as forecasting, earthquake prediction, etc.

For tracking a dynamic target, the pose estimation from two CCD cameras is defined as $x(t)$, where t = 1, 2,…, n, and the accumulated generating operation is defined as the accumulated measurements $z(k) = \Sigma_{t=1}^{k} x(t)$ for (k =1, 2,..., n). The dynamic change of $z(t)$ is modeled by the following first-order ordinary differential equation:

$$dz(t)/dt + az(t) = b. \tag{12}$$

In grey theory, (12) is called the "white descriptor" for modeling a white system; the corresponding parameters a and b can be estimated from the poses of two CCD cameras. For effectiveness, equation (12) is approximated by the following grey-differential equation:

$$dz(t)/dt + ag(t) = b \tag{13}$$

where $g(t) = (z(t+1) + z(t))/2$. Then the least-squares method is employed to obtain the optimal parameters by introducing the accumulated generating operation in a time interval. The first term of (13) in a discrete system can be written as

$$dz(t)/dt = z(t+1) - z(t) = x(t+1) \tag{14}$$

where the sampling time of measurements is taken as a unit. In addition, equation (13) can be rewritten as

$$x(t+1) = -0.5a[z(t+1) + z(t)] + b. \tag{15}$$

Substituting the sequential data x and z into (15) gives

$$Y = B\Phi \tag{16}$$

where $Y = [x(2) \quad x(3) \quad \cdots \quad x(n)]^T$, $B \in \Re^{(n-1)\times 2}$, $n > 2$, with

its row vector j, $B_j = \left[-0.5(z(j+1)+z(j)) \quad 1\right]$, and $\Phi = \left[a \quad b\right]^T$. Then the following quadratic equation is defined for the cost function of the least squares method.

$$J = (Y - B\Phi)^T (Y - B\Phi). \tag{17}$$

The optimal solution can be obtained by minimizing the J using the matrix derivation ∇ with respect to Φ as the following equations:

$$\nabla_\Phi J = 2\left[\nabla_\Phi (Y - B\Phi)^T\right]\left[Y - B\Phi\right] \tag{18}$$

$$\nabla_\Phi (Y - B\Phi)^T = -\nabla_\Phi \Phi^T B^T = -B^T. \tag{19}$$

Setting (18) to zero, the optimal parameters of the grey model is obtained as follows:

$$\hat{\Phi} = \left[\hat{a} \quad \hat{b}\right]^T = (B^T B)^{-1} B^T Y. \tag{20}$$

The estimated parameters are then brought into the response solution of the first-order ordinary differential equation (12) for the prediction of the accumulated generating operation:

$$\hat{z}(n+1) = \left[z(1) - \hat{b}/a\right] e^{-an} + \hat{b}/a. \tag{21}$$

Different orders or variables of grey model can refer to some references, e.g., [22, 23].

4. EXPERIMENTS AND DISCUSSIONS

There are two subsections to discuss the experiments. The subsection 4.1 is the experimental preliminaries including pose estimation and strategy of tracking modes. The second subsection arranges three representative experiments.

4.1 Experimental Preliminaries

1) *Pose Estimation*

First, two sets of three LEDs with different light areas are placed to suitable locations of the tracking car and the target car, respectively. Then three corresponding points on the image plane to represent three positions with respect to world coordinate (i.e., $(\hat{x}_1, \hat{y}_1), (\hat{x}_2, \hat{y}_2)$, and $(\hat{x}_3, \hat{y}_3)$ in Fig. 2) are obtained. Based on the relation (22)-(24), the world coordinate of the tracking car and the target car at geometry center is then attained.

$$\theta(k) = \tan^{-1}\left\{\left[\hat{y}_1(k) - \left(\hat{y}_2(k) + \hat{y}_3(k)\right)/2\right] \Big/ \left[\hat{x}_1(k) - \left(\hat{x}_2(k) + \hat{x}_3(k)\right)/2\right]\right\} \tag{22}$$

$$\hat{x}(k) = \left(2\hat{x}_1(k) + \hat{x}_2(k) + \hat{x}_3(k)\right)/4 \tag{23}$$

$$\hat{y}(k) = \left(2\hat{y}_1(k) + \hat{y}_2(k) + \hat{y}_3(k)\right)/4. \tag{24}$$

In addition, the image system to detect the response of the tracking and target cars is introduced as follows. The interpolation method is employed to obtain the relationship between the world coordinate and the image coordinate. Because a CCD camera does not face squarely to a plane in the world coordinate, an image of plane in the world coordinate becomes a trapezium (the length of upper side and lower side is 225c*m*, and 145c*m*, respectively, and the depth is 300c*m*). Due to the distortion of image plane, a straight line on image plane is shown as an oblique line in the world coordinate. Similarly, a straight line in the world coordinate becomes an oblique line on the image plane. There is an overlap with width 24c*m* between the ends of two trapezoid areas. The control authority in this overlap region is according to the distinguishable error; higher distinguishable error indicates higher control authority to monitor the tracking car or the target car. The centerline of the overlap is set as the equal control authority for the corresponding two CCD cameras. The maximum estimation error is about 2*cm*, which is acceptable and merely occurs in the periphery of the trapezoid.

According to the restriction of grabbing frequency for a CCD camera, the sampling time for the image processing and trajectory planning is set as 130*ms*. While the tracking car or that target car is in the left trapezoid area, the related pose is estimated by CCD1. After trajectory planning, the reference command for the tracking car is sent by a wireless device. Similarly, as the tracking car or the target car is in the right trapezoid area, the corresponding pose is estimated by CCD2; the planned reference command is also sent by the same wireless device. However, when the tracking car or the target car is inside the overlap region, two CCD cameras can grab the image and the corresponding pose is estimated either by CCD1 or CCD2.

2) *Strategy of Target Tracking Modes*

From the very beginning, various definitions for the strategy of the target tracking are given in Fig. 6. These definitions are described as follows: (i) L_c (unit: *cm*) denotes the distance between the centers of the tracking car and the target car, (ii) L_s (unit: *cm*) denotes the safe distance to avoid the bump of the target car by the tracking car, (iii) the point d represents the desired pose of the tracking car with a safe distance from the center of the

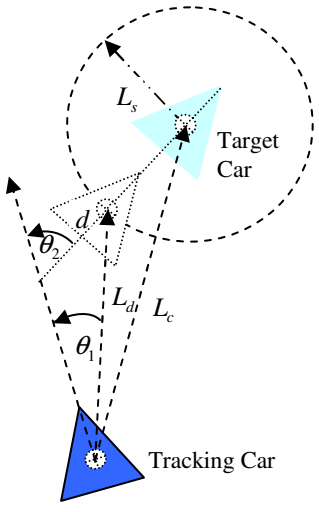

Fig. 6. Definitions for the strategy of target tracking.

target car and the same orientation of the target car, (iv) L_d (unit: *cm*) denotes the distance between the center of the tracking car and the point *d*, (v) θ_1 (unit: degree) denotes the angle between the orientation of the tracking car and the direction of the tracking car with respect to the desired target pose, and (vi) θ_2 (unit: degree) stands for the angle between the orientation of the tracking car and the direction of the tracking car with respect to the desired target pose. In addition, the tracking car and target car respectively depict in the color of dark blue and light blue. The angles for θ_1 and θ_2 are positive as it is in a counterclockwise direction. The normal velocity of the target car is assumed to be $1.2rps$ or $37.7\,cm/s$, which is about 60% of the highest velocity in this experiment. There are eight tracking modes in this study. Due to the symmetrical feature (i.e., the tracking car can be in the right-hand and left-hand sides of the target car), only 4 different modes (i.e., the tracking car is the left-hand side of the target car) are introduced as follows:

(1) The target car is in the front of the tracking car, and their orientation is consistent. It is so-called "tracking mode 1" (refer to Fig. 7). The numbers 1,2,3,... with symbols *square* and *circle* represent the sequences of the tracking car and the target car, respectively. In this situation, the reference steering angle for the front-wheel (i.e., $\sigma_{r_1}(t)$ or $\phi_r(t)$) is assigned as follows (see Fig. 8(a)):

$$\sigma_{r_1}(t)=\begin{cases}-\theta_1, & \text{if } L_d>10,\\ -\theta_2, & \text{otherwise,}\end{cases} \quad \text{where} -30^\circ \le \theta_1,\theta_2 \le 30^\circ.$$

Simultaneously, the reference velocity for the rear-wheel (i.e., $\sigma_{r_2}(t)$ or $v_r(t)$) is assigned in Fig. 8(b) with $l_0=15, l_1=55, l_2=60$ and $l_3=100\,cm$. The details of this tracking mode can be referred to Fig. 7.

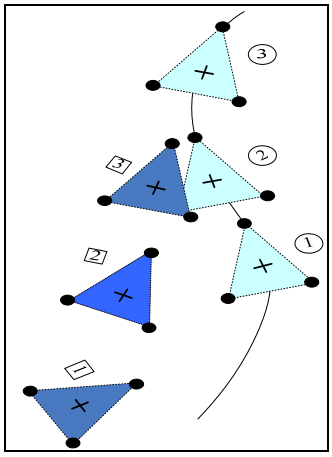

Fig. 7. Tracking mode 1.

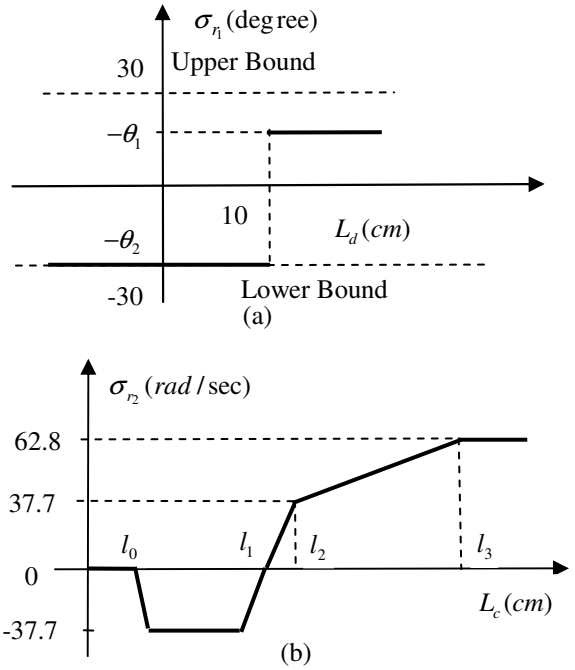

Fig. 8. The reference steering angle for the front-wheel and the reference velocity for the rear-wheel of tracking mode 1.

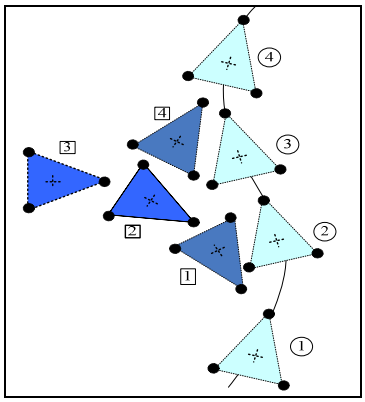

Fig. 9. Tracking mode 2.

(2) The target car is in the preceding of the tracking car, and their orientation is opposite. It is so-called "tracking mode 2" (allude to Fig. 9). The tracking car will be backward with the reference velocity -37.7 or $-62.8cm/\sec$, which is inversely proportional to the distance L_c, and simultaneously turn right with the reference steering angle, e.g., -30 degree. After a few seconds, the reference velocity and the reference steering angle for the tracking car are simultaneously assigned $37.7cm/\sec$ and 30 degree, respectively; i.e., the tracking car is commanded with the motion of forward and left-turn. Then the situation of the tracking

and target cars is in the "tracking mode 1." Sequentially, the operation of the tracking car will follow the strategy of "tracking mode 1."

(3) The target car is at the back of the tracking car, and their orientation is consistent. It is so-called "tracking mode 3" (refer to Fig. 10). The tracking car will be forward with the reference velocity 37.7 or $62.8cm/\sec$, which is inversely proportional to the distance L_c, and simultaneously turn right with the reference steering angle, e.g., -30 degree. After a few seconds, the reference velocity and the reference steering angle for the tracking car are simultaneously assigned $-37.7cm/\sec$ and 30 degree, respectively; i.e., the tracking car is commanded with the motion of backward and left-turn. Until the tracking car and the target are in the situation of "tracking mode 1", the sequential operation of the tracking car will follow the strategy of "tracking mode 1."

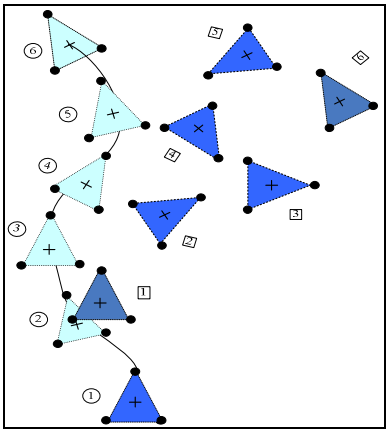

Fig. 10. Tracking mode 3.

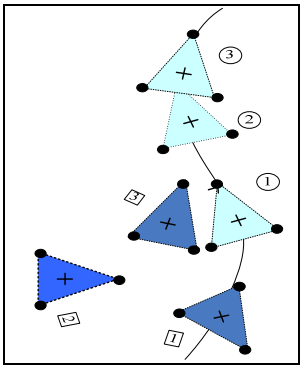

Fig. 11. Tracking mode 4.

(4) The target car is at the back of the tracking car and their orientation is opposite. It is so-called "tracking mode 4" (allude to Fig.11). The tracking car will be backward with the reference velocity 37.7 or $62.8cm/\sec$, which is inversely proportional to the distance L_c, and simultaneously turn right with the reference steering angle, e.g., -30 degree. After a few seconds, the reference velocity and the reference steering angle for the tracking car are simultaneously assigned $37.7cm/\sec$ and 30 degree, respectively; i.e., the tracking car is commanded with the motion of forward and left-turn. Then the situation of the tracking and target cars is in the "tracking mode 1." Sequentially, the operation of the tracking car will follow the strategy of "tracking mode 1."

Based on these strategies for tracking a target car, the following subsection will show three representative cases of our experiments.

4.2 Experimental Results

The responses of PID control and the proposed control for the unloaded condition (e.g., the tracking car does not contact with ground) are similar. For simplicity, those are omitted. However, the loaded response will be poor as compared with the proposed fuzzy decentralized sliding-mode control [29]. Therefore, only the FDSMC is applied to the tracking car for the target tracking in sensor-network environment.

Because the subsystem of steering angle is a type one system [30], its control input is the output of fuzzy table (i.e., Table 3) multiplied an output scaling factor g_{311}, i.e., an absolute control. On the other hand, the 2nd subsystem is a velocity control system, i.e., a type zero system [30]. To eliminate the steady-state error of 2nd subsystem, an integrator is used for the output of fuzzy table (i.e., Table 3) multiplied an output scaling factor; i.e., 2nd subsystem is an incremental control system. Alternatively, the 2nd subsystem can be supposed to be a velocity control system with an integrator. In the beginning, the coefficients for the switching surface are chosen as follows: $G_1 = diag\{3125, 125\}$ and $G_2 = diag\{12.5, 0.5\}$. The responses of the front-wheel and rear-wheel for different reference steering angles (i.e., ϕ_r) and reference velocities (i.e., v_r) by using the scaling factors $G_s = G_2, G_{\dot{s}} = 50I_2$, and $G_3 = 6I_2$, are all in a satisfactory manner. For brevity, those are omitted. In general, the values of G_s and $G_{\dot{s}}$ have the influence on the output scaling factor G_3; the larger values of G_s or $G_{\dot{s}}$ implies larger value of G_3. The tracking results are satisfactory; these signals are also smooth enough.

Due to the gear ratio of the steering subsystem is 190:1, the torque for driving the steering angle is enough. Hence, the scaling factors for this subsystem are the same as those in the unloaded tracking car. Because the 2nd subsystem is employed to drive the tracking car, the corresponding scaling factors are larger than those in the unloaded

tracking car. In summary, the following scaling factors $G_s = G_2$, $G_{\dot{s}} = diag\{50, 300\}$, and $G_3 = 6I_2$ are selected. Similarly, the coefficients for the switching surface are chosen as $G_1 = diag\{3125, 300\}$ and $G_2 = diag\{12.5, 1.2\}$, which possess a larger value in the 2nd subsystem as compared with the unloaded case.

Because the target car is dynamic and the tracking car possesses dynamics, a grey prediction (refer to subsection 3.2) for the pose of the target car is employed to plan an *effective* reference command for the tracking car to enhance the performance of target tracking. In the beginning, the target car moves with a curve of "8", this is remotely controlled by a human. Then the tracking car using FDSMC is employed to track the target car. The related response is shown in Fig. 12 (a), which is acceptable. At the same time, a grey prediction together with fuzzy decentralized sliding-mode control (i.e., FDSMGPC) is applied for the above-mentioned case. For simplicity, only *GM*(1,1) grey model is applied to predict the pose of the target car. The corresponding response is presented in Fig. 12(b). Because the target car and the tracking car possess dynamics, an FDSMGPC indeed improves the system performance as compared with FDSMC. In fact, the faster motion of the target car moves, the predicted effect is more dominant. However, the dynamic target tracking is not merely the prediction problem. Faster motion of the target car will be difficult to track. Hence, a compromise should be made. In addition, different orders or variables for the grey model can be considered to enhance the prediction (e.g., see [22, 23]).

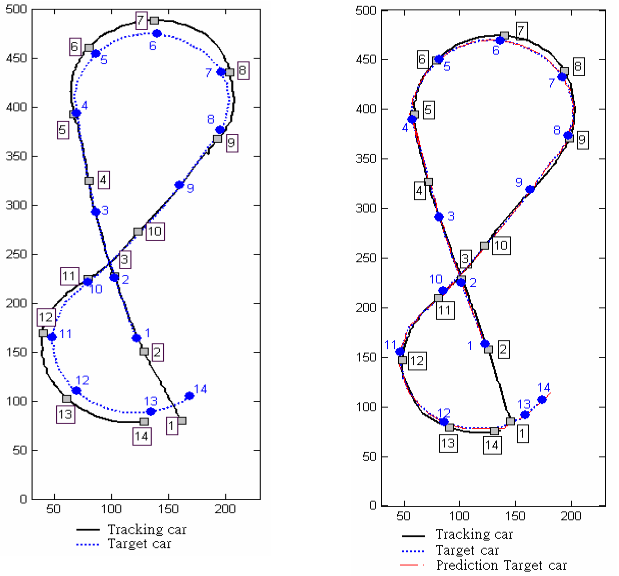

(a) (b)

Fig.12. Experimental result of target tracking. (a) Without using grey prediction. (b) Using grey prediction.

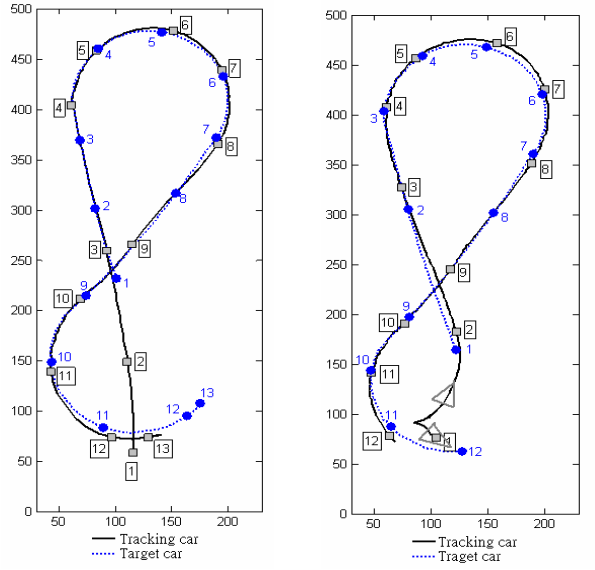

(a) (b)

Fig. 13. Figure 12(b) case. (a) Two seconds delay of tracking car. (b) Different initial pose of tracking car.

To demonstrate the effectiveness, the target tracking of Fig. 12(b) case is verified by different initial time (e.g., two seconds delay as compared with Fig. 12(b)). The corresponding response is shown in Fig. 13 (a). Finally, the response of Fig. 12(b) case for different initial pose of the tracking car is depicted in Fig. 13(b). These responses are all in a satisfactory manner. The responses for the other motion of target tracking, e.g., faster movement of target car, different control parameters, are similar with Figs. 12 and 13; for brevity, those are left out. Although the reference commands for the tracking car are given every 130*ms*, the control cycle time of two driven motors for the tracking car is 10*ms*. Therefore, the bandwidth of the tracking car is still large enough for high-frequency movement to track the target car.

5. CONCLUSIONS

The proposed control system included two processors (i.e., one DSP and one PC) with multiple sampling rates (i.e., 10*ms* and 130*ms*). A smaller sampling time is for the control of the tracking car; on the other hand, a larger sampling time is for the planning of the reference command of the tracking car. Therefore, the bandwidth of the tracking car is still large enough to manipulate a high-frequency motion for dynamic target tracking. No mathematical model for the little known tracking car is needed to design a controller. In the beginning, the values of G_1 and G_2 are chosen to stabilize the sliding surface with appropriate dynamics. The scaling factors G_s and $G_{\dot{s}}$ are employed to normalize the sliding surface and its derivative. Based on the system stability, the output scaling factor G_3 is chosen. Although the discontinuity and poor quality of image system in the vicinity of the overlap region

and the periphery of sensor-network environment occur, the satisfactory tracking performance of dynamic target consolidates the usefulness of the proposed control system. Furthermore, total eight tracking modes for target tracking are planned and executed by our car-like wheeled robots. The authors are supposed that these tracking modes can be a method for the problem of dynamic target tracking. If the monitoring region is larger, the number of the CCD cameras should be increased or active CCD camera should be considered [11]. If the outdoor application of tracking and target cars is considered, a GPS is applied to replace the CCD cameras [24].

6. REFERENCES

[1] Sinopoli, B., Sharp, C., Schenato, L., Schaffert, S. and Sastry, S. S., "Distributed control applications within sensor networks", *Proceedings of the IEEE,* Vol. 91, No. 8, 2003, pp. 1235-1246.

[2] Yamaguchi, T., Sato, E. and Takama, Y., "Intelligent space and human centered robotics", *IEEE Trans. Ind. Electron.*, Vol. 50, No. 5, Oct. 2003, pp. 881-889.

[3] Lee, J. H. and Hashimoto, H., "Controlling mobile robots in distributed intelligent sensor network", *IEEE Trans. Ind. Electron.*, Vol. 50, No. 5, Oct. 2003, pp. 890-902.

[4] Doctor, F., Hagras, H. and Callaghan, V., "A fuzzy embedded agent-based approach for realizing ambient intelligence in intelligent inhabited environments", *IEEE Trans. Syst. Man & Cyber., Part A*, Vol. 35, No. 1, Jan. 2005, pp. 55-65.

[5] Briechle, K. and Hanebeck, U. D., "Location of a mobile robot using relative bearing measurements", *IEEE Trans. Robot. & Automat.*, Vol. 20, No. 1, Feb. 2004, pp. 36-44.

[6] Luo, R. C. and Chen, T. M., "Autonomous mobile target tracking system based on grey fuzzy control algorithm", *IEEE Trans. Ind. Electron.*, Vol. 47, No. 4, Aug. 2004, pp. 920-931.

[7] Yang, S. X. and Meng, Q. H., "Real-time collision-free motion planning of a mobile robot using a neural dynamics-based approach", *IEEE Trans. Neural Networks*, Vol. 14, No. 6, Nov. 2003, pp. 1541-1552.

[8] Yang, S. X., Li, H., Meng, M. Q.-H. and Liu, P. X., "An embedded fuzzy controller for a behavior-based mobile robot with guaranteed performance", *IEEE Trans. Fuzzy Syst.*, Vol. 12, No. 4, Aug. 2004, pp. 436-446.

[9] Minguez, J. and Montano, L., "Nearness diagram (ND) navigation: collision avoidance in troublesome scenarios", *IEEE Trans. Robot. & Automat.*, Vol. 20, No. 1, Feb. 2004, pp. 45-59.

[10] Li, T. H. S. and Chang, S. J., "Fuzzy target tracking control of autonomous mobile robots by using infrared sensors", *IEEE Trans. Fuzzy Syst.,* Vol. 12, No. 4, Aug. 2004, pp. 491-501.

[11] Hwang, C. L., Shih, C. Y. and Wong, C. C., "A distributed active-vision network-space approach for trajectory tracking and obstacle avoidance of a car-like wheeled robot", *IEEE FUZZ2007*, London, England, pp. 1-6, July 10th- 13th, 2007.

[12] Tseng, C. S. and Chen, B. S. H_∞ decentralized fuzzy model reference tracking control design for nonlinear interconnected systems. *IEEE Trans. Fuzzy Syst.*, Vol. 9, No. 6, Dec. 2001, pp. 795-809.

[13] Feddema, J. T., Lewis, C. and Schoenwald, D. A., "Decentralized control of cooperative robotic vehicles: theory and application", *IEEE Trans. Robotics & Automation*, Vol. 18, No. 5, Oct. 2002, pp. 852-864.

[14] Hwang, C. L. and Hsu, C. W., "A thin and deep hole drilling using a fuzzy discrete sliding mode control with a woodpeckering strategy", *IME Proc. J. Syst., Contr. Eng*, Vol. 209, 1995, pp. 281-291.

[15] Baturone, I. Moreno-Velo, F. J., Sanchez-Solano, S., and Ollero, A.., "Automatic design of fuzzy controllers for car-like autonomous robots", *IEEE Trans. Fuzzy Syst.*, Vol. 12, No. 4, Aug. 2004, pp. 447-465.

[16] Lin, W. C., Huang, C. L. and Chuang, M. K., "Hierarchical fuzzy control of autonomous navigation of wheeled robots", *IEE Proc.-D, Control Theory & Appl.*, Vol. 152**,** No**.** 5, Oct. 2005, pp. 598-606.

[17] Young, D., Utkin, V. I. and Özgüner, Ü., "A control Engineer's guide to sliding mode control", *IEEE Trans. Contr. Syst. Technol.*, Vol. 7, No. 3, May 1999, pp. 328-342.

[18] Hwang, C. L., "Neural-network-based variable structure control of electrohydraulic servosystems subject to huge uncertainties without the persistent excitation", *IEEE/ASME Trans. Mechatron.,* Vol. 4, No. 1, Jan. 1999, pp. 50-59.

[19] Hwang, C. L. and Chang, L. J., "Internet-based fuzzy decentralized microprocessor control for a two-dimensional piezo-driven system," *IEEE SMC2006*, Taipei, Taiwan, Vol. 4, pp. 3080-3085, October 8-11th, 2006.

[20] Goodwin, G. C. and Sin, K. S., Adaptive filtering prediction and control, Prentice-Hall Inc. 1984,

[21] Jitao, L., Chengfa, W., Dasong, X. and Peigang, L., "Application of grey system theory to the forecasting and control of air environment quality", *J. Grey Syst.*, Vol. 4, 1992, pp. 181–192.

[22] Tien, T. L., "The indirect measurement of tensile strength of material by the grey prediction model GMC(1,n)", *J. of Meas. Sci. Technol.*, Vol. 16, 2005, pp. 1322-1328.

[23] Tien, T. L., "A research on the prediction of machine accuracy by the deterministic grey dynamic model DGDM(1,1,1)", *Appl. Math. & Comp*., Vol. 161, 2005, pp. 923-945.

[24] Valavanis, K. P., Doitsidis, L. and Murphy, R. R., "A

case study of fuzzy-logic-based robot navigation", *IEEE Robotics & Automation Magazine*, September, 2006, pp. 93-107.

[25] Hwang, C. L., Wang, T. H. and Wong, C. C., "A dynamic target tracking of wheeled robot in sensor-network environment via fuzzy decentralized sliding-mode grey prediction control", *IEEE ICRA2007*, Roma, Italy, pp. 3463-3469, April 10th-14th , 2007.

[26] Fierro, R. and Lewis, F. L., "Control of a nonholonomic mobile robot using neural networks", *IEEE Trans. Neural Networks*, Vol. 9, No. 4, Jul. 1998, pp. 589-600.

[27] Rigatoos, G. G., Tzafestas, S. G. and Evangelidis, G. J., "Reactive parking control of nonhomolonomic vehicles via a fuzzy learning automation", *IEE Proc., Control Theory Appl.*, Vol. 148**,** No**.** 2, Apr. 2001, pp. 169-179.

[28] Wang, L. X., *A course in fuzzy systems and control*, Prentice-Hall Inc., 1997.

[29] Hwang, C. L., Yu, Y. S. and Han, S. Y., "A network-based fuzzy decentralized sliding-mode control for car-like mobile robots", *IEEE Trans. Ind. Electron.*, Vol. 54, No. 1, Feb. 2007, pp. 574-585.

[30] Kuo, B. C., *Automatic control*, Prentice-Hall Inc. 8th Ed., 2006.

APPENDIX

Define the following Lyapunov function:

$$V(t) = S^T(t)S(t)/2 > 0, \quad \text{as } S(t) \neq 0. \tag{A1}$$

Taking the time derivative of eqn. (A1), substituting eqns. (6)-(8), (11), (9) and (10) into eqn. (A2), and using the fact $G_2A^{-1}D > 0$, yields

$$\begin{aligned}
\dot{V} &= S^T\left\{G_1\left[\dot{R}-\dot{Y}\right]+G_2\left[\ddot{R}+A^{-1}\left(B+C+\Gamma-DU\right)\right]\right\} \\
&= S^T\left\{F-G_2A^{-1}DU\right\} \\
&= S^TF - S^TG_2A^{-1}DG_3\left[S+\Delta\operatorname{sgn}(S)\right] \qquad \text{(A2)} \\
&\le \|S\|\textstyle\sum_{i=1}^{2}\left\{f_i\right| - g_{2m}g_{3ii}\delta_{ii}/(a_Md_M)\} \\
&\le -\|S\|\textstyle\sum_{i=1}^{2}\{\lambda_i\} \le -\lambda\|S\| = -\lambda\sqrt{2V}, \quad \lambda = \min(\lambda_1,\lambda_2).
\end{aligned}$$

Then, the solution of the inequality (A2) for the initial time t_0 and the initial value $S(t_0)$ is described as follows:

$$t - t_0 \le \|S(t_0)\|/\lambda \tag{A3}$$

where t stands for the time that the operating point hits the sliding surface (i.e., $S(t) = 0$), and $t - t_0$ denotes the finite time to approach the sliding surface. Once the operating point reaches the stable sliding surface (6), the tracking error asymptotically converges to zero.

Q.E.D.

Chih-Lyang Hwang received the B.E. degree in Aeronautical Engineering from Tamkang University, Taiwan, R.O.C., in 1981, the M.E. and Ph.D. degree in Mechanical Engineering from Tatung Institute of Technology, Taiwan, R.O.C., in 1986 and 1990, respectively.

From 1990 to 2006, he had been with the Department of Mechanical Engineering of Tatung Institute of Technology (or Tatung University), where he was engaged in teaching and research in the area of servo control and control of manufacturing systems and robotic systems. He was a Professor of Mechanical Engineering of Tatung Institute of Technology (or Tatung University) from 1996 to 2006. During 1998-1999, he was a research scholar of George W. Woodruf School of Mechanical Engineering of Georgia Institute of Technology, USA. Since 2006, he is a Professor of the Department of Electrical Engineering of Tamkang University, Taiwan, R.O.C. He is the author or coauthor of about 100 journal and conference papers in the related field. His current research interests include navigation of mobile robot, fuzzy (or neural-network) modeling and control, variable structure control, robotics, visual tracking system, network-based control, and distributed sensor-network.

Dr. Hwang received a number of awards, including the Excellent Research Paper Award from the National Science Council of Taiwan and Hsieh-Chih Industry Renaissance Association of Tatung Company. From 2003 to 2006, he was one of the Committee in Automation Technology Program of National Science Council of Taiwan, R.O.C. He was a Member of Technical Committee of the 28th Annual Conference of the IEEE Industrial Electronics Society.

Tsai-Hsiang Wang received the B.E. degree from Feng-Chia University, Taichung, Taiwan, R.O.C., in 2003, and the master degree from Tatung University, Taipei, Taiwan, R.O.C., in 2005. All is in Mechanical Engineering.

His current research interests include the navigation of mobile robot and fuzzy control. Now, he is in a military service.

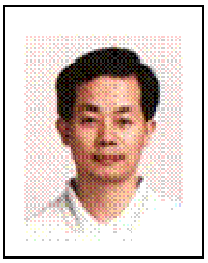

Ching-Chang Wong received a B.S. degree in Electronic Engineering from Tamkang University, Taipei Hsien, Taiwan, in 1984. He received a M.S. and a Ph.D. degree in Electrical Engineering from the Tatung Institute of Technology, Taipei, Taiwan, in 1986 and 1989, respectively. He joined the Electrical Engineering Department of Tamkang University in 1989 and now is a professor. His research interests include fuzzy systems, intelligent control, SOPC design, and robot design.